Efficient passively *Q*-switched Yb:LuAG microchip laser

Jun Dong,[1,*] Ken-ichi Ueda,[1] and Alexander A. Kaminskii[2]

[1]*Institute for Laser Science, University of Electro-Communications, 1-5-1 Chofugaoka, Chofu, Tokyo 182-8585, Japan*
[2]*Institute of Crystallography, Russian Academy of Sciences, Leninsky Prospekt 59, Moscow 119333, Russia*
**Corresponding author: dong@ils.uec.ac.jp*

Received August 24, 2007; revised October 8, 2007; accepted October 9, 2007;
posted October 15, 2007 (Doc. ID 86824); published November 2, 2007

An efficient passively *Q*-switched Yb:LuAG microchip laser with Cr^{4+}:YAG as saturable absorber was demonstrated for the first time to our knowledge. Slope efficiencies of 40% and 28% were measured for the initial transmission of Cr^{4+}:YAG, T_0=95% and 90%, respectively. Laser pulses with a pulse energy of 19 μJ and a pulse width of 610 ps at the repetition rate of 12.8 kHz were achieved for T_0=90%; the corresponding peak power of over 31 kW was obtained. The lasers oscillated at two or three longitudinal modes owing to the broad emission spectra of Yb:LuAG and mode selection by Cr^{4+}:YAG thin plate acting as an intracavity etalon. © 2007 Optical Society of America

OCIS codes: 140.3380, 140.3480, 140.3540, 140.5680.

Among more than 230 oxide and fluoride laser host-crystalline materials, the lutetium compounds (at present ~30 species) are of special interest for solid-state lasers [1]. In particular, the substitution of Lu^{3+} ions for Y^{3+} ions in several structures, such as $Lu(WO_4)_2$ [2], $LuVO_4$ [3], and $Lu_3Al_5O_{12}$ (LuAG) [4,5] provides Lu compounds with preferable conditions for trivalent lanthanide (Ln^{3+}) lasant doping. Lu laser crystals are a special chapter in modern material science. Passively *Q*-switched lasers of Yb^{3+}-doped laser crystals (Yb:YAG [6], Yb:GdAB [7], Yb:NaGdW [8], and so on) with Cr^{4+}:YAG as saturable absorber have been demonstrated. Yb:LuAG crystals have become one of the important solid-state laser materials because they have a large effective emission peak cross section compared to that of the Yb:YAG crystal [5]. Yb:LuAG also has mechanical properties, such as high thermal conductivity, comparable to that of Yb:YAG crystal [9]. The other particularly important characteristic of Yb:LuAG crystal is that it has very strong absorption at 970 nm, which is higher than that at 940 nm. Therefore, high quantum efficiency can be achieved by using a 970 nm laser diode (LD) as a pumping source. Optical properties of Yb:LuAG and LD-pumped Yb:LuAG lasers were reported at room temperature [5]. Temperature-dependent laser performance of Yb:LuAG crystals under 970 nm LD pumping was also performed [10]. More recently, crystal growth, spectroscopic, and laser properties of Yb:LuAG crystals doped with various Yb concentrations were investigated [9]. The results show that Yb:LuAG will be more suitable for ultrashort pulse generation. Here, we report, for the first time to our knowledge, on the experimental investigations of LD end-pumped low-threshold, highly efficient, and compact passively *Q*-switched Yb:LuAG microchip lasers by using Cr^{4+}:YAG saturable absorbers.

Figure 1 shows a schematic of a passively *Q*-switched Yb:LuAG/Cr^{4+}:YAG microchip laser. A plane-parallel, 1.12 mm thick LuAG crystal plate (C_{Yb}=8.2 at. %, 6 mm×6 mm cross section) was used as the gain medium. One surface of the Yb:LuAG plate is antireflection coated at 940 nm and highly reflecting at 1030 nm to act as a cavity mirror. The other surface is antireflection coated at the 1030 nm lasing wavelength to reduce the cavity loss. Two uncoated 0.5 mm thick Cr^{4+}:YAG crystals with different initial transmissions (T_0=95% and 90%) were used as a *Q* switch. The saturated transmissions of these two Cr^{4+}:YAG crystals are 99%, and 97.5% for T_0=95%, and 90%, as determined by measuring the transmission of Cr^{4+}:YAG under the intense laser pulse at 1064 nm. The Cr^{4+}:YAG crystal was tightly sandwiched between the Yb:LuAG plate and a plane-parallel output coupler with 20% transmission. The total cavity length was 1.62 mm. The choice of 20% transmission of the output coupler (OC) is based on a theoretical analysis of a *Q*-switched laser [11–13] and is also helpful in avoiding coating damage by reducing the intracavity laser intensity. A high-power fiber-coupled 940 nm LD with a core diameter of 100 μm and numerical aperture of 0.22 was used as the pump source. Two lenses with 8 mm focal lengths were used to focus the pump beam on the Yb:LuAG lasing crystal rear surface and to produce a pump light spot in the crystal of ~100 μm in diameter. The *Q*-switched pulse shapes and pulse trains were recorded by using a fiber-coupled InGaAs photodiode with a bandwidth of 16 GHz (rise time from 10% to 90% is 25 ps), and a 7 GHz Tektronix TDS7704B digital oscilloscope. The spectral composition of these la-

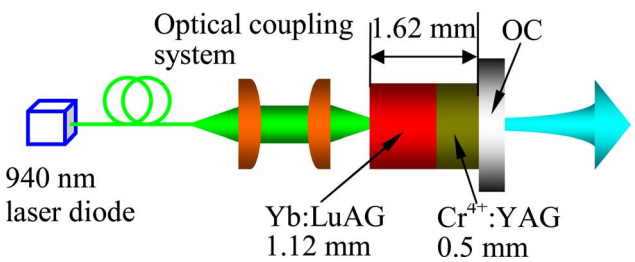

Fig. 1. (Color online) Schematic of LD end-pumped passively *Q*-switched Yb:LuAG/Cr^{4+}:YAG microchip lasers.

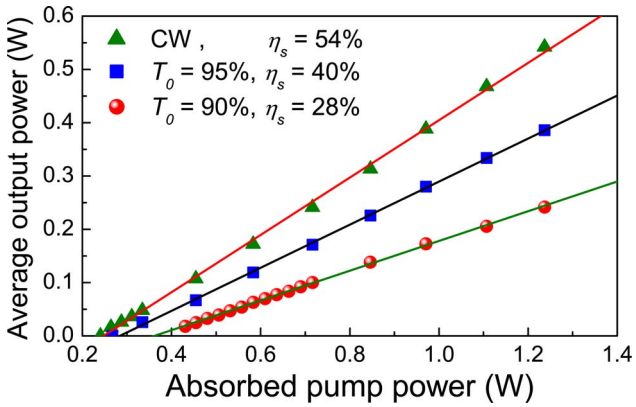

Fig. 2. (Color online) Average output power of passively Q-switched Yb:LuAG microchip lasers as a function of the absorbed pump power for T_0=95, and 90% together with cw output power. The solid lines show the linear fits of the experimental data.

sers was analyzed with an optical spectrum analyzer (ANDO AQ6137). The laser output beam profile was monitored using a CCD camera both in the near field and the far field of the OC.

The continuous-wave (cw) operation of Yb:LuAG microchip laser was performed ahead of the passively Q-switched laser experiments. The absorbed pump power for reaching laser threshold was 240 mW, the slope efficiency was over 54%. A 542 mW output power was obtained when the absorbed pump power was 1.24 W, and the corresponding optical-to-optical efficiency was 44%. The average output power as a function of absorbed pump power for passively Q-switched Yb:LuAG/Cr^{4+}:YAG microchip lasers is shown in Fig. 2, together with the cw output power. The pump power thresholds were ~0.26 and 0.42 W for T_0=95% and 90%, respectively. The average output power increases linearly with absorbed pump power for different T_0 of Cr^{4+}:YAG saturable absorber. There was no pump saturation; the output power can be further scaled with high pump power. The slope efficiencies (η_s) were measured to be ~40% and 28% for T_0=95% and 90%, respectively. A maximum average output power of 386 mW was measured when the absorbed pump power was 1.24 W for T_0 =95%. The corresponding optical-to-optical efficiency of 31% was achieved for T_0=95%. For T_0=90%, the corresponding optical-to-optical efficiency was ~19.5%. The decrease of the efficiency of passively Q-switched lasers with the low initial transmission of Cr^{4+}:YAG is due to the strong absorption of excited state absorption of Cr^{4+}:YAG crystals [14]. However, the pulse energy will be increased and pulse width will be shortened with the low initial transmission of Cr^{4+}:YAG crystals [13]. In practice, the initial transmission of Cr^{4+}:YAG can be chosen to realize the different pulse energy and repetition rate, depending on the applications of such lasers.

The cw laser operates in a TEM_{00} mode with multilongitudinal modes (three to five) owing to the broad emission spectra of Yb:LuAG crystal. Stimulated emission (SE) indicated that this passively Q-switched Yb:LuAG/Cr^{4+}:YAG microchip laser oscillates in two or three longitudinal modes, depending on the pump power level. The fundamental mode radius close to the output coupler for these lasers was measured to be 55 μm. Figure 3 shows the SE spectra of cw and Q-switched Yb:LuAG microchip lasers with T_0=90% Cr^{4+}:YAG as saturable absorber under different pump power levels. Two longitudinal modes were obtained when the absorbed pump power was kept below 0.8 W. Three longitudinal modes dominated at a high pump power regime (e.g., P_{abs} >0.8 W). The separation between each mode was measured to be 0.525 nm, which is two times wider than those of cw oscillation and three times wider than the free spectral range ($\Delta\lambda_c$=0.18 nm) in the laser cavity filled with gain medium predicted by [15] $\Delta\lambda_c=\lambda^2/2L_c$, where L_c is the optical length of the resonator and λ is laser wavelength. The cause of wide separation between each mode is attributed to the intracavity tilted etalon effect of the Cr^{4+}:YAG thin plate [15]. The mode linewidth FWHM was less than 0.02 nm, limited by the resolution of the optical spectra analyzer. The central wavelength of cw and Q-switched lasers shifts to a longer wavelength, which is caused by the temperature dependent emission spectrum of the Yb:LuAG crystal, which is similar to the case of the Yb:YAG crystal [16]. Under the same absorbed pump power level, the emitting wavelength of Q-switched lasers shifts to a longer wavelength compared to that of the cw case. This was caused by the high intracavity intensity of the Q-switched laser, which is in good agreement with the previous report of the wavelength shift of Yb^{3+}:Y_2O_3 laser [17].

Figure 4 shows the pulse energy, pulse repetition rate, pulse width, and peak power as a function of the absorbed pump power for two values of T_0 of the Cr^{4+}:YAG saturable absorbers. Pulse energy increases with the absorbed pump power and pulse energy tends to be saturated when the absorbed pump power is higher than 0.6 W. The repetition rate increases linearly with absorbed pump power. The error bars indicate the increase of timing jitter at a high repetition rate, and the timing jitter is less than 5% even at a high pump power. The pulse width decreases slowly with the absorbed pump power. Peak

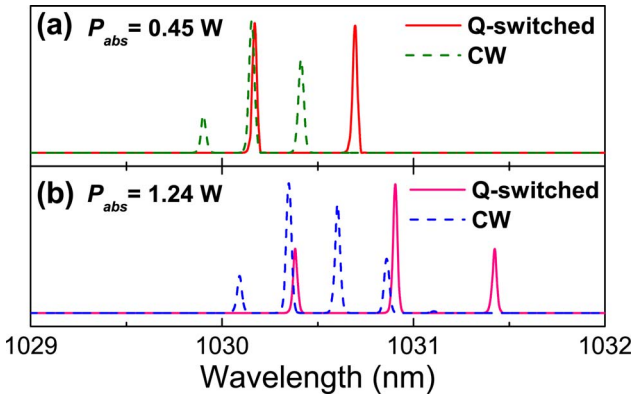

Fig. 3. (Color online) Comparison of stimulated emitting spectra of cw and passively Q-switched Yb:LuAG microchip lasers under different pump power levels.

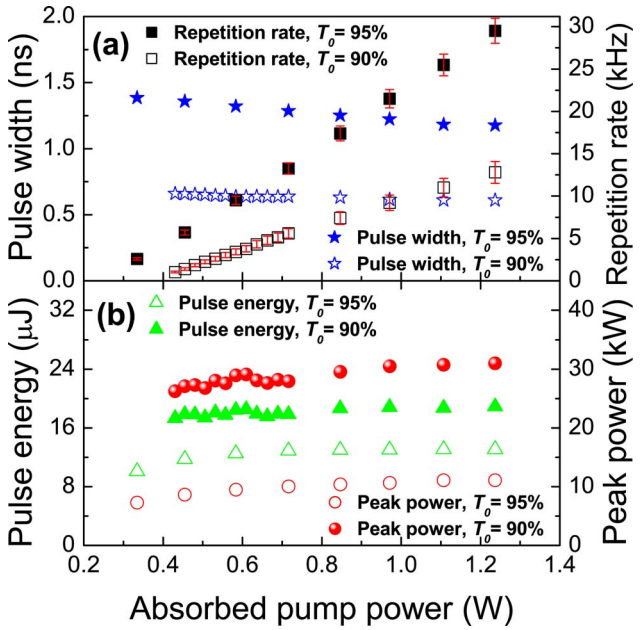

Fig. 4. (Color online) Pulse characteristics (pulse energy, pulse width, repetition rate, and peak power) of LD end-pumped passively Q-switched Yb:LuAG microchip lasers as a function of absorbed pump power.

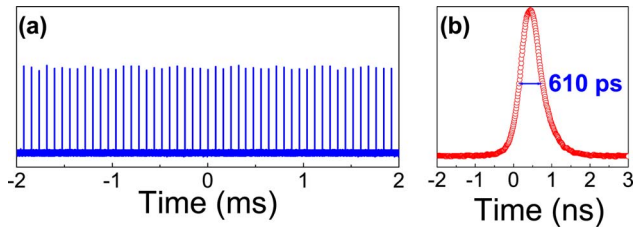

Fig. 5. (Color online) (a) Oscilloscope trace of pulse trains, (b) laser pulse with 610 ps pulse width and pulse energy of 19 μJ, corresponding to peak power of over 31 kW.

power increases with absorbed pump power and tends to saturate at a high pump power level. Typical pulse trains and pulse profiles for T_0=90% are shown in Fig. 5. The output pulse amplitudes and timing jitter are less than 5% [as shown in Fig. 5(a)], evidencing a very stable passively Q-switching laser operation. Over 31 kW laser pulses with a pulse width of 610 ps were obtained at a repetition rate of 12.8 kHz when the absorbed pump power is 1.24 W [as shown in Fig. 5(b)]. As can been seen from the laser pulse characteristics of passively Q-switched Yb:LuAG/Cr^{4+}:YAG microchip lasers, the Yb:LuAG crystal is very easily saturated by inserting Cr^{4+}:YAG. The pulse energy, pulse width, and peak power are nearly independent of the pump power, which is in good agreement with the theoretical prediction [11].

Passively Q-switched Yb:LuAG/Cr^{4+}:YAG microchip lasers have been demonstrated for the first time. A slope efficiency of 40% and optical-to-optical efficiency of 31% at 1.03 μm lasing wavelength were achieved by using T_0=95% Cr^{4+}:YAG crystal. Laser pulses with a 610 ps pulse width and a 19 μJ pulse energy at 1.03 μm have been obtained by using T_0 =90% Cr^{4+}:YAG crystal, which corresponds to the peak power of over 31 kW. Wide-separated ($\Delta\lambda_c$ =0.525 nm) multilongitudinal mode oscillation due to the Cr^{4+}:YAG thin plate acting as an etalon was obtained, depending on the pump power level.

This work was supported by the 21st Century Center of Excellence (COE) program of the Ministry of Education, Science, Sports, and Culture of Japan. A. A. Kaminskli acknowledges the Russian Foundation for Basic Research and the Russian Academy of Sciences.

References

1. A. A. Kaminskii, Laser Photonics Rev. **1**, 93 (2007).
2. J. Liu, U. Griebner, V. Petrov, H. Zhang, J. Zhang, and J. Wang, Opt. Lett. **30**, 2427 (2005).
3. J. Liu and V. Petrov, Opt. Lett. **31**, 3294 (2006).
4. G. A. Bogomolova, D. N. Vylegzhanin, and A. A. Kaminskii, Sov. Phys. JETP **42**, 440 (1976).
5. D. S. Sumida, T. Y. Fan, and R. Hutcheson, in *OSA Proceedings on Advanced Solid-State Lasers* (Optical Society of America, 1995), p. 348.
6. J. Dong, A. Shirakawa, and K. Ueda, Appl. Phys. B **85**, 513 (2006).
7. A. Brenier, C. Tu, Z. Zhu, and J. Li, Appl. Phys. Lett. **90**, 071103 (2007).
8. J. Liu, V. Petrov, H. Zhang, J. Wang, and M. Jiang, Opt. Lett. **32**, 1728 (2007).
9. A. Brenier, Y. Guyot, H. Canibano, G. Boulon, A. Rodenas, D. Jaque, A. Eganyan, and A. G. Petrosyan, J. Opt. Soc. Am. B **23**, 676 (2006).
10. T. Kasamatsu, H. Sekita, and Y. Kuwano, Appl. Opt. **38**, 5149 (1999).
11. J. J. Degnan, IEEE J. Quantum Electron. **31**, 1890 (1995).
12. J. J. Degnan, in *Proceedings of the 10th International Workshop on Laser Ranging Instrumentation* (Chinese Academy of Sciences, 1996), p. 334.
13. J. J. Degnan and J. J. Zayhowski, in *Proceedings of the 11th International Workshop on Laser Ranging*, (Federal Office for Cartography and Geodesy, Germany, 1998), p. 453.
14. Z. Burshtein, P. Blau, Y. Kalisky, Y. Shimony, and M. R. Kokta, IEEE J. Quantum Electron. **34**, 292 (1998).
15. W. Kochner, *Solid State Laser Engineering*, 5th ed. (Springer-Verlag, 1999).
16. J. Dong, M. Bass, Y. Mao, P. Deng, and F. Gan, J. Opt. Soc. Am. B **20**, 1975 (2003).
17. J. Kong, D. Y. Tang, J. Lu, and K. Ueda, Opt. Lett. **29**, 65 (2004).